UCSF

UC San Francisco Previously Published Works

Title

Flow patterns in the jugular veins of pulsatile tinnitus patients

Permalink

https://escholarship.org/uc/item/8h6453wr

Authors

Kao, Evan

Kefayati, Sarah

Amans, Matthew R

et al.

Publication Date

2017-02-01

DOI

10.1016/j.jbiomech.2016.12.008

Peer reviewed

eScholarship.org Powered by the California Digital Library
University of California

Author Manuscript

Author Manuscript

Author Manuscript

Author Manuscript

HHS Public Access

Author manuscript

*J Biomech*. Author manuscript; available in PMC 2018 February 08.

Published in final edited form as:

*J Biomech*. 2017 February 08; 52: 61–67. doi:10.1016/j.jbiomech.2016.12.008.

# Flow Patterns in the Jugular Veins of Pulsatile Tinnitus Patients

**Evan Kao**[1,2], **Sarah Kefayati**[2], **Matthew R. Amans**[2], **Farshid Faraji**[2], **Megan Ballweber**[2], **Van Halbach**[2], and **David Saloner**[2]

[1]Department of Bioengineering, UC Berkeley, Berkeley, CA, USA

[2]Department of Radiology and Biomedical Imaging, UCSF, San Francisco, CA, USA

## Abstract

Pulsatile Tinnitus (PT) is a pulse-synchronous sound heard in the absence of an external source. PT is often related to abnormal flow in vascular structures near the cochlea. One vascular territory implicated in PT is the internal jugular vein (IJV). Using computational fluid dynamics (CFD) based on patient-specific Magnetic Resonance Imaging (MRI), we investigated the flow within the IJV of seven subjects, four symptomatic and three asymptomatic of PT. We found that there were two extreme anatomic types classified by the shape and position of the jugular bulbs: elevated and rounded. PT patients had elevated jugular bulbs that led to a distinctive helical flow pattern within the proximal internal jugular vein. Asymptomatic subjects generally had rounded jugular bulbs that neatly redirected flow from the sigmoid sinus directly into the jugular vein. These two flow patterns were quantified by calculating the length-averaged streamline curvature of the flow within the proximal jugular vein: $130.3 \pm 8.1\ m^{-1}$ for geometries with rounded bulbs, $260.7 \pm 29.4\ m^{-1}$ for those with elevated bulbs ($P < 0.005$). Our results suggest that variations in the jugular bulb geometry lead to distinct flow patterns that are linked to PT, but further investigation is needed to determine if the vortex pattern is causal to sound generation.

### Keywords

Pulsatile Tinnitus; Computational Fluid Dynamics; Magnetic Resonance Imaging

## 2. Introduction

A variety of imaging modalities are available to evaluate abnormalities of the intracranial venous circulation including CT Angiography, MR Angiography, and catheter-based diagnostic cerebral angiography. These methods afford detailed images of the geometric morphology of veins that are frequently tortuous with highly varying caliber. However, these anatomic studies provide little insight into the flow patterns of blood within these veins.

Corresponding author: Evan Kao, SF VA Medical Center, 4150 Clement St., Building 203 Room BA-33, San Francisco, CA 94121, Phone: 415-221-4810 ext. 23801, evan.kao@ucsf.edu.

**Conflict of Interest Statement**: There are no conflicts of interest to declare.

**Publisher's Disclaimer:** This is a PDF file of an unedited manuscript that has been accepted for publication. As a service to our customers we are providing this early version of the manuscript. The manuscript will undergo copyediting, typesetting, and review of the resulting proof before it is published in its final citable form. Please note that during the production process errors may be discovered which could affect the content, and all legal disclaimers that apply to the journal pertain.

Author Manuscript Author Manuscript Author Manuscript Author Manuscript

Understanding flow patterns in the cerebral veins could provide important information about the pathophysiology of many clinical conditions. This report focuses on the venous flow patterns in patients with pulsatile tinnitus (PT).

Tinnitus is the auditory perception of sound in the absence of an external source. It affects more than 50 million Americans, often severely (Krishnan et al., 2006). It is not uncommon for patients to suffer from insomnia, depression, or even suicidal ideations (Jacques et al., 2013; Pridmore et al., 2012). A small subset of tinnitus (5-10%), termed PT, is pulsatile and is often described as a “whooshing” sound (Harvey et al., 2014; Liyanage et al., 2006). PT is often related to abnormal flow in vascular structures near the cochlea (Krishnan et al., 2006; Madani and Connor, 2009). PT etiologies can be venous (40%), arterial (35%), or undetermined (25%) (Mattox and Hudgins, 2008).

While controversial, abnormal internal jugular vein (IJV) geometries, such as enlarged or high-riding jugular bulbs (HJB), have been suggested as a source of PT in a subset of patients. A cohort study (Sonmez et al., 2007) found that subset to be roughly 30% of PT patients, though we note their study did not correlate symptom laterality with the side of the venous abnormality. Case studies (Adler and Ropper, 1986; Buckwalter et al., 1983; Chandler, 1983) proposed that the blood flow through the anatomic aberration may contribute to PT. Patients reported changes in PT with changes in flow through the jugular vein; for example, decreased flow with ipsilateral neck compression led to decreased symptoms, while increased flow in high-flow states (e.g. exercise or pregnancy) have been linked to increased pulsatile tinnitus strength (Buckwalter et al., 1983).

Despite those observations, we emphasize that an association between PT and abnormal jugular bulbs is only tentative. Both Buckwalter et al. (1983) and Chandler (1983) promoted jugular vein ligation as a treatment for PT, which has since been determined ineffective (Jin and Wang, 2015). Additionally, the presence of a HJB alone is not itself predictive of PT; Marsot-Dupuch (2001) determined that only 4.5% of patients with an enlarged jugular bulb ever develop PT, while Park et al. (2015) found a 35% prevalence of HJB in patients with hearing loss. The ambiguity of the role of abnormal jugular vein geometries and flow rate in PT pathology suggests the link between flow, shape, and sound, if it exists, must be complex; simply observing the flow rate and bulb shape is not enough to identify the origin of venous PT.

This study was motivated by our preliminary observations of complex flow within the jugular vein (Acevedo-Bolton et al., 2015; Kefayati et al., 2016). Those studies reveal a pronounced vortex core surrounded by a peripheral circulating flow pattern. Similar geometries and flow patterns have been noted by others as a source of sound (Vonnegut, 1954). We believe more detailed and subcategorized analyses are needed to define the relationship between the structure of the cerebral venous system and the flow patterns, which in turn may help elucidate the source of PT.

Bony structures overlying the draining veins limit the use of Doppler Ultrasound, the conventional *in vivo* approach for measuring velocities. MR velocimetry overcomes this limitation through its ability to define the full velocity vector in three-dimensional space

Author Manuscript Author Manuscript Author Manuscript Author Manuscript

throughout the pulsatile cycle – a method referred to as 4D MR Velocimetry (4D-MRV) (Markl et al., 2012; Nayak et al., 2015). 4D-MRV has been explored in application to the cerebral venous sinuses for both *in vivo* and *in vitro* models (Acevedo-Bolton et al., 2015, Kefayati et al., 2016). However, 4D-MRV is restricted in both spatial and temporal resolution. Furthermore, *in vivo* measurement only evaluates the specific physiologic condition presented at time of examination, and cannot readily explore flow field variations in response to different physiological conditions, such as heart rate or exercise, that might alter total volume flow.

Compared to *in vivo* MRV, Computational Fluid Dynamics (CFD) provides higher spatial and temporal resolution, and parameters can be adjusted to explore physiologic limits. We therefore employed CFD to provide controlled simulations in the complex anatomic geometries of the transverse sinus (TS), sigmoid sinus (SS), and internal jugular vein (IJV). This work utilized subject-specific CFD based on lumenal geometries from contrast-enhanced MR Venography (MRV), and inlet flow waveforms from 2D through-plane MR velocimetry measured for each individual. As a starting point, we investigated the relationship between jugular geometry and flow by comparing the velocity fields in “elevated” jugular bulbs, which were prevalent in our symptomatic population, to those in “rounded” bulbs, which were prevalent in our asymptomatic subjects.

## 3. Materials and Methods

### 3.1 Subject Recruitment

Subjects were recruited from the UCSF Pulsatile Tinnitus Clinic and provided informed consent for participation in accordance with the procedures approved by our Institutional Review Board. Subjects with unrelated pathology known to cause PT were excluded from analysis (Table 1).

### 3.2 Image Acquisition

Imaging was performed on a 3T Siemens Skyra (Siemens Medical Systems, Erlangen, Germany) and consisted of a high-resolution MR venogram to define the venous lumenal geometry, and MR flow studies to define the inlet flow volume through each SS.

The MRV consisted of a large volume 3D Contrast-Enhanced MR Angiography (CE-MRA) study acquired at 0.7mm isotropic resolution. A timing run using a 2cc bolus of GdDTPA delivered at 2cc $s^{-1}$ followed by a 15cc saline flush at 2cc $s^{-1}$ was performed. Injection was initiated simultaneously with low-resolution 3D volume studies acquired at 1 second intervals. The time delay, $T_{delay}$, between injection and arrival of the contrast in the jugular vein was determined from visual inspection of the resulting maximum intensity projection images. The full contrast bolus of 20cc Gd followed by a 15cc saline flush, all injected at 2cc $s^{-1}$, was then delivered and the high-resolution 3D CE-MRA was acquired beginning at $T_{delay}$ after the start of injection. The 3D volume consisted of a coronal slab, 124 mm thick using a total acquisition time of 45 seconds. Imaging parameters were: $T_R$ = 3.66 s; $T_E$ = 1.4 s; Flip angle = 20°; FOV = 200 mm; Matrix = 320 × 240; number of slices = 172; acceleration factor = 3.

Author Manuscript Author Manuscript Author Manuscript Author Manuscript

Inlet flow waveforms were measured using retrospective, pulse-gated, 2D Phase-Contrast (PC)-MR Velocimetry. Through-plane velocities were measured for planes prescribed transverse to each SS. Parameters of the 2D PC MR were: slice thickness = 5 mm; $T_R$ = 37 s; $T_E$ = 3.6 s; Flip angle = 20°; cardiac phase length = 40 ms; VENC = 100 cm $s^{-1}$; FOV = 200 mm; Matrix = 256 × 154; acceleration factor = 2.

### 3.3. Jugular Bulb Classification

The geometry of each subject's jugular bulb on the symptomatic side was classified by a board-certified Neuroradiologist (MRA). In symptomatic patients, the index side was defined as the side where symptoms of PT were most acutely perceived. For the asymptomatic “control” subjects, the index side was defined as that of the dominant draining vein based on mean flow measured by 2D PC-MR. The geometry was categorized as either “elevated” or “rounded” (Figure 1). “Elevated” was defined as having the apex of the jugular bulb raised above the roof of the SS at its inlet into the IJV, whereas “rounded” was defined by the absence of any pronounced ascent in the jugular bulb and a smoother transition into the jugular vein. We note that our definition for “elevated” geometries does not follow the standard clinical definition for HJB. When assignment to one of those two categories was ambiguous, the anatomy was categorized as “neither”.

### 3.4. Simulation

For each subject, a surface representation of the SS and IJV from the relevant side was segmented from the CE-MRA data using the Vascular Modeling Toolkit (VMTK) (Orobix, Bergamo, Italy) and Geomagic Design X (Geomagic, Rock Hill, USA). Flow extensions were provided at the inlets (the entrance to the SS) to ensure developed flow. Tetrahedral meshes from the surfaces were generated (also in VMTK) with a targeted edgelength of 0.6mm, resulting in meshes of approximately 200,000 nodes and 1,000,000 cells. The edgelength was chosen by repeating simulations for edgelengths varying from 0.4mm to 1.0mm on one selected jugular geometry. 0.6mm was found optimal as finer meshes did not result in any noticeable differences in major flow features.

Simulations were performed using FLUENT (ANSYS, Canonsburg, USA). Assumptions included a rigid wall, a Newtonian fluid, and laminar flow. A coupled solver was used with second-order pressure and second-order momentum discretization schemes. The fluid material was defined to resemble blood at body temperature, with a density of 1060 kg $m^{-3}$ and a viscosity of 0.0035 kg $m^{-1}s^{-1}$. A zero-pressure condition was prescribed at the outlet. Flow profiles were extracted from the 2D-MRV data using Segment (Medviso AB, Lund, Sweden) (Bidhult et al., 2014). For one representative case from each geometric group, two simulations were performed: One with pulsatile flow using the measured flow waveform, and one with steady flow using the peak flow value. Those results demonstrated that the dominant flow features found for pulsatile flow were noted at peak systole, and that the steady flow simulation reflected the same features. We therefore limited our analyses to steady flow at peak systole.

Author Manuscript Author Manuscript Author Manuscript Author Manuscript

### 3.5. Flow Pattern Analysis

Initial inspection of the velocity fields indicates that the flow patterns of “elevated” and “rounded” jugular bulbs differed in the presence and extent of downstream helical flow, and by the presentation of vortex cores. In order to visualize the vortex cores, swirling strength values were calculated throughout the volume and displayed in Paraview (Kitware, New York, USA). The flows were quantified by calculating the length-averaged streamline curvatures within the proximal jugular vein to provide a well-defined single parameter indicative of flow shape.

The streamlines were generated forwards and backwards in time and visualized in Paraview, using seed points dispersed throughout the geometry. For each streamline, the curvature at each point was numerically calculated according to

$$\kappa = \left\| \frac{\partial \boldsymbol{T}}{\partial s} \right\| \quad (1)$$

where the curvature $\boldsymbol{\kappa}$, is defined as the derivative of the tangent vector $\boldsymbol{T}$ with respect to the line's parameterization $s$. Streamlines were manually cut to a region of interest approximately 1.5cm along the length of the vessel's centerline that included the jugular bulb and the proximal jugular vein (Figure 2).

The length-averaged streamline curvatures were then calculated as

$$C = \frac{1}{L} \sum_{i}^{N} \int_{l_i} \kappa_i(s) ds, \qquad L = \sum_{i}^{N} l_i \quad (2)$$

where the curvatures for all streamlines are integrated with respect to length and divided by $L$, the total length of all streamlines. The number of streamlines $N$ is chosen to provide a value of $C$ that is insensitive to changes in $N$ (Figure 3).

### 3.6. Statistical Analysis

Statistical significance between two subject groups was determined using Welch's t-test, which is more reliable than the Student's t-test when comparing groups with different sample sizes and variances.

## 4. Results

16 individuals were recruited: 12 subjects who reported symptoms of PT and 4 controls (for summary, see Table 1). Of the symptomatic subjects, two were excluded due to underlying pathology known to cause PT (namely fistulas and SS diverticulum). One PT patient reported congenital unilateral deafness, and was excluded from further analysis due to inability to reliably lateralize the symptomatic side. Of the remaining nine PT patients, six

Author Manuscript Author Manuscript Author Manuscript Author Manuscript

were classified as having “neither” geometry, three had elevated bulbs, and none had rounded bulbs. Of the four controls, one had elevated bulbs and three had rounded bulbs.

Mean and peak flows for the patient and control groups are provided in Table 2. Also included are Reynolds numbers calculated at the junction between the SS and the jugular bulb.

### 4.1 Characterizing flow patterns by visualizing vortex cores

Flow patterns for all rounded and elevated geometries are provided in Figures 4 and 5. Flow patterns in rounded geometries are characterized by a strong component of flow that travels from the sigmoid sinus directly down the center of the proximal jugular vein. Remaining flow that enters from the sigmoid sinus creates prominent vortex cores in the dilated proximal jugular bulb that propagate along the walls of the bulb parallel to the central stream. For elevated geometries, the presence of the arch of the jugular bulb above the sigmoid sinus results in a small component of flow being directed to the apex of the jugular bulb that then subsequently spirals down the center of the bulb. The remaining major component of flow enters the proximal jugular vein at a right angle from the sigmoid sinus, creating a large helical flow structure that rotates about the central spiral. This can be represented by a large vortex core encompassing the proximal jugular vein, which typically increases in strength in the distal IJV, where the vein narrows.

### 4.2 Quantifying flow patterns by length-averaged streamline curvature

Evaluation of the quantitative metrics of the velocity fields for all subjects with elevated jugular bulb anatomies and for subjects with rounded jugular bulbs also reflected these differences. Inspection of the streamlines and swirling strength distributions reveal that their values are strongly associated with each type of geometry.

The presence or absence of the two flow patterns can be differentiated quantitatively by calculating the length-averaged streamline curvature within the proximal jugular vein, essentially marking the presence (greater curvature) or absence (lesser curvature) of the characteristic helical flow pattern previously described. Figure 6 provides the length-averaged streamline curvatures for both types of jugular bulb shapes, while Figure 7 depicts the relevant streamlines colored by local streamline curvature for all subjects. Rounded bulbs lead to flows with length-averaged streamline curvatures of $130.3 \pm 8.1\ m^{-1}$, while elevated bulbs have length-averaged streamline curvatures of $260.7 \pm 29.4\ m^{-1}$. These values are statistically significant for $P < 0.005$.

## 5. Discussion

### 5.1 Image-based velocity field evaluation

This study expands on findings from an *in vivo* imaging study of the velocity field patterns in the jugular veins of patients with PT (Acevedo-Bolton et al., 2015), but the current work includes a greater number of patients and utilizes CFD. Similar to the work of Acevedo-Bolton and colleagues, we also found the velocity field in subjects with elevated jugular bulbs to be extremely complex with pronounced vortical components. We demonstrate

Author Manuscript Author Manuscript Author Manuscript Author Manuscript

differences in the vortical component of flow between jugular veins with elevated and rounded bulbs that can be both observed and quantified. We hypothesize the vortical component plays a role in sound generation in PT.

The methods outlined by this work are minimally invasive, requiring a small injection of contrast agent during MRI to provide images with sufficient resolution to construct a computational mesh for accurate CFD simulation of important flow features. The approach described here suggests *in vivo* MR imaging can be used across a broad range of venous anatomies and provide the boundary conditions required for detailed CFD analysis of velocity fields on a patient-specific basis.

### 5.2 Pathophysiology of pulsatile tinnitus in the jugular vein

Our study is an exploratory step toward investigating the possible impact of the blood flow velocity field on the pathophysiology of PT thought to be originating in the jugular vein. Our results suggest a relationship between geometry, flow, and PT. The differences in flow in the jugular veins of subjects with elevated bulbs and those with rounded bulbs can be distinguished both visually and quantitatively.

HJB is an established clinical entity that has been proposed to contribute to PT (Dietz et al., 1994; Madani and Connor, 2009; Sismanis, 2003; Sonmez et al., 2007; Vattoth et al., 2010). In our work, symptomatic subjects had a higher incidence of elevated jugular bulb geometries. This study indicates that elevated jugular bulbs can result in a distinct flow pattern that has a large component of vortical flow in the proximal jugular vein.

Audible bruits are detected in stenotic carotid arteries where downstream vortices shed from turbulent flow are thought to be the source of the flow-induced sound. Similarly, vortical instabilities and pressure fluctuations induced near the lumen wall have been described as a source of audible sound that can be auscultated at the aortic root (Seo et al., 2013). While arterial stenosis and Seo's work explicitly reference unstable flow, the results presented here are expected to represent stable flow due to the low, steady flow rates imposed. Nevertheless, several considerations argue that flow in these territories might have associated unsteady flow and pressure fluctuations related to the same geometrical factors that determine the extent of swirling flow revealed by our simulations. The elevated bulb anatomy can be described as a narrow vessel (the SS) that expands into the elevated bulb and drains into the distal IJV, which is often strongly tapered. An analogy can be drawn to the “vortex whistle” geometry, investigated by Vonnegut (1954) and Chanaud (1963), which can be described as a tangential inlet leading into a cylindrical cavity that drains into a smaller downstream tube. Those studies showed that even steady flow through the geometry resulted in an unstable vortex that generated a characteristic whistle. Additionally, the expansion of the SS into the jugular bulb may create flow instabilities that lead to oscillations in the pressure fields, particularly in the apex of the bulb. Furthermore, physiological flow is never perfectly steady, and physiological variability, e.g. breathing and cardiac pulsatility, may perturb total flow and induce pressure fluctuations on the wall. These considerations indicate that conditions that result in vortical flow may also produce audible sound. These sources of sound remain speculative and identifying acoustic sources is a subject of ongoing study.

Author Manuscript Author Manuscript Author Manuscript Author Manuscript

Sound generation in the jugular bulb could be amplified by its physiology. The jugular bulb is the only portion along the SS and IJV that lacks adventitia and it lies near the inner ear space, which contains the cochlea (Buckwalter et al., 1983). Raised jugular bulbs are in close apposition to the temporal bone and the middle ear space. The temporal bone is structured for optimal sound transmission, and waves emanating from the jugular bulb could pass directly into the temporal bone and be readily transmitted to the cochlea. The low amplitude of sound waves generated may account for the difficulty examiners have in appreciating venous PT on auscultation.

### 5.3 Limitations

Conclusions are limited by the small sample size. Furthermore, in this initial analysis, we have simplified the distribution of anatomical presentations to either elevated or rounded. While this analysis serves to clearly differentiate velocity patterns between these two presentations, there is a much broader variation found in the general population. Furthermore, subject inclusion into the “elevated” geometry did not require meeting typical definitions of HJB to the level of the floor of the internal auditory canal (Vachata et al., 2010). The relationship of PT to jugular bulb morphology is likely to be more complex than binary anatomic divisions such as what we and others have used.

This study presents a correlation between highly vortical flow and elevated bulb geometry, but does not establish that vortical flow is directly responsible for PT. The purpose of this study was to investigate whether a relationship exists between jugular bulb anatomy and the presence of a strong vortex component of flow. Further studies are required to determine if the relationship is causal in nature.

The CFD simulations performed here were based on several assumptions. We did not include models of non-Newtonian flow, which may be reasonable for the large caliber jugular bulb, but could be inaccurate for stenosed veins. Imposing rigid walls could also affect the flow field. Distension along the sigmoid sinus is limited by the dura, skull, and intracranial pressure. The jugular bulb is often partly surrounded by bone that limits distension. Time-resolved cine images from the 2D-MRV data at 0.5 mm in-plane spatial resolution and 40ms temporal resolution revealed no discernable distension of the wall over the cardiac cycle in our region of interest (the SS and proximal IJV). However, *in vivo* imaging does reveal some distension in the cervical jugular vein. One approach to assess the effect of wall motion would be to compare velocity fields computed by CFD with *in vivo* cardiac cycle time-resolved 4D-MR flow measurements, a study that we are pursuing at this time.

Another limitation of our study is that we did not consider the effects of patient posture (e.g., lying or standing) on the geometry of the jugular vein, which could be important due to vessel compressibility. However, that is partially mitigated in this study, since both subject groups were lying supine during imaging.

Author Manuscript Author Manuscript Author Manuscript Author Manuscript

## 6. Conclusions

Our study identifies a strong correlation between anatomic morphology of the jugular bulb and resulting flow patterns. Elevated jugular bulbs present with a pronounced vortex. A possible connection between conditions that promote the type of vortical flow and the generation of sound is postulated, but a definitive causal mechanism remains to be established.

## Acknowledgments

Financial support for this project was provided by the Department of Radiology and Biomedical Imaging, UCSF. Grant support was provided by the NIH, HL114118 (DS) and NS059944 (DS).

## References

Acevedo-Bolton G, Amans MR, Kefayati S, Halbach V, Saloner D. Four dimensional magnetic resonance velocimetry for complex flow in the jugular vein. Quantitative Imaging in Medicine and Surgery. 2015; 5(4):635–7. [PubMed: 26435930]

Adler JR, Ropper AH. Self-audible venous bruits and high jugular bulbs. Archives of Neurology. 1986; 43(3):257–259. [PubMed: 3947273]

Bidhult, S., Carlsson, M., steding-Ehrenborg, K., Arheden, H., Heiberg, E. A new method for vessel segmentation based on a priori input from medical expertise in cine phase-contrast Magnetic Resonance Imaging. Proceedings of Seventeenth Annual SCMR Scientific Sessions; New Orleans, USA. 2014.

Buckwalter JA, Sasaki CT, Virapongse C, Kier EL, Bauman N. Pulsatile Tinnitus arising from jugular megabulb deformity. Laryngoscope. 1983; 93(12):1534–1539. [PubMed: 6645753]

Chanaud RC. Experiments Concerning the Vortex Whistle. The Journal for the Acoustical Society of America. 1963; 35(7):953–960.

Chandler JR. Diagnosis and cure of venous hum tinnitus. Laryngoscope. 1983; 93(7):892–895. [PubMed: 6865626]

Dietz RR, Davis WL, Harnsberger HR, Jacobs JM, Blatter DD. MR imaging and MR angiography in the evaluation of pulsatile tinnitus. American Journal of Neuroradiology. 1994; 15(5):879–89. [PubMed: 8059655]

Harvey RS, Hertzano R, Kelman E, Eisenman DJ. Pulse-synchronous tinnitus and sigmoid sinus wall anamolies: descriptive epidemiology and the idiopathic intracranial hypertension patient population. Otology & Neurotology. 2014; 35(1):7–15. [PubMed: 24270723]

Jacques D, Nozeret Y, Zdanowicz N, Reynaert C, Garin P, Gilain C. Tinnitus and psychiatric comorbidities in liaison psychiatry analysis of three years in an audiophonology center. Psychiatria Danubina. 2013; 25(2):S102–4. [PubMed: 23995155]

Jin L, Wang Y. Management of venous pulsatile tinnitus with normal otoscopic findings. Ear, Nose & Throat Journal. 2015; 94.9:386, 388, 390, 392.

Kefayati S, Amans M, Faraji F, Ballweber M, Kao E, Ahn S, Meisel K, Halbach V, Saloner D. The Manifestation of Vortical and Secondary Flow in the Cerebral Venous Outflow Tract: An In Vivo MR Velocimetry Study. Journal of Biomechanics. 2016 in press.

Krishnan A, Mattox DE, Fountain AJ, Hudgins PA. CE arteriography and venography in pulsatile tinnitus: preliminary results. American Journal of Neuroradiology. 2006; 27(8):1635–8. [PubMed: 16971601]

Liyanage SH, Singh A, Savundra P, Kalan A. Pulsatile tinnitus. Journal of Laryngology and Otology. 2006; 120(2):93–7. [PubMed: 16359136]

Madani G, Connor SE. Imaging in pulsatile tinnitus. Clinical Radiology. 2009; 64(3):319–28. [PubMed: 19185662]

Markl M, Frydrychowicz A, Kozerke S, Hope M, Wieben O. 4D flow MRI. Journal of Magnetic Resonance Imaging. 2012; 36:1015. [PubMed: 23090914]

Author Manuscript Author Manuscript Author Manuscript Author Manuscript

Marsot-Dupuch K. Pulsatile and non-pulsatile tinnitus: a systemic approach. Seminars in Ultrasound, CT and MRI. 2001; 22(3):250–270.

Mattox DE, Hudgins P. Algorithm for evaluation of pulsatile tinnitus. Acta Oto-Laryngologica. 2008; 128(4):427–31. [PubMed: 18368578]

Nayak KS, Nielsen JF, Bernstein MA, Markl M, Botnar RM, Gatehouse PD, Saloner D, Lorenz C, Wen H, Hu BS, Epstein FH, Oshinski JN, Raman SV. Cardiovascular magnetic resonance phase contrast imaging. Journal of Cardiovascular Magnetic Resonance. 2015; 17:71. [PubMed: 26254979]

Park JJH, Shen A, Loberg C, Westhofen M. The relationship between jugular bulb position and jugular bulb related inner ear dehiscence: a retrospective analysis. American Journal of Otolaryngology. 2015; 36(3):347–351. [PubMed: 25701459]

Pridmore S, Walter G, Friedland P. Tinnitus and suicide: recent cases on the public record give cause for reconsideration. Otolaryngolology – Head and Neck Surgery. 2012; 147(2):193–5.

Seo JH, Vedula V, Abraham T, Mittal R. Multiphysics computational models for cardiac flow and virtual cardiography. International Journal for Numerical Methods in Biomedical Engineering. 2013; 29(8):850–869. [PubMed: 23666911]

Sismanis A. Pulsatile Tinnitus. Otolaryngologic Clinics of North America. 2003; 36(2):389–402. viii. [PubMed: 12856306]

Sonmez G, Basekim CC, Ozturk E, Gungor A, Kizilkaya E. Imaging of pulsatile tinnitus: a review of 74 patients. Clinical Imaging. 2007; 31(2):102–8. [PubMed: 17320776]

Vachata P, Petrovicky P, Sames M. An anatomical and radiological study of the high jugular bulb on high-resolution CT scans and alcohol-fixed skulls of adults. J Clin Neurosci. 2010; 17(4):473–8. [PubMed: 20167495]

Vattoth S, Shah R, Curé JK. A compartment-based approach for the imaging evaluation of tinnitus. American Journal of Neuroradiology. 2010; 31(2):211–8. [PubMed: 19762464]

Vonnegut B. A Vortex Whistle. The Journal of the Acoustical Society of America. 1954; 26(1):16–20.

Author Manuscript Author Manuscript Author Manuscript Author Manuscript

**Figure 1.**
MIP images of the vasculature around the internal jugular vein. The arrows point to the geometry of interest, the jugular bulb, for a rounded bulb (*Left*) and a raised bulb (*Right*).

Author Manuscript Author Manuscript Author Manuscript Author Manuscript

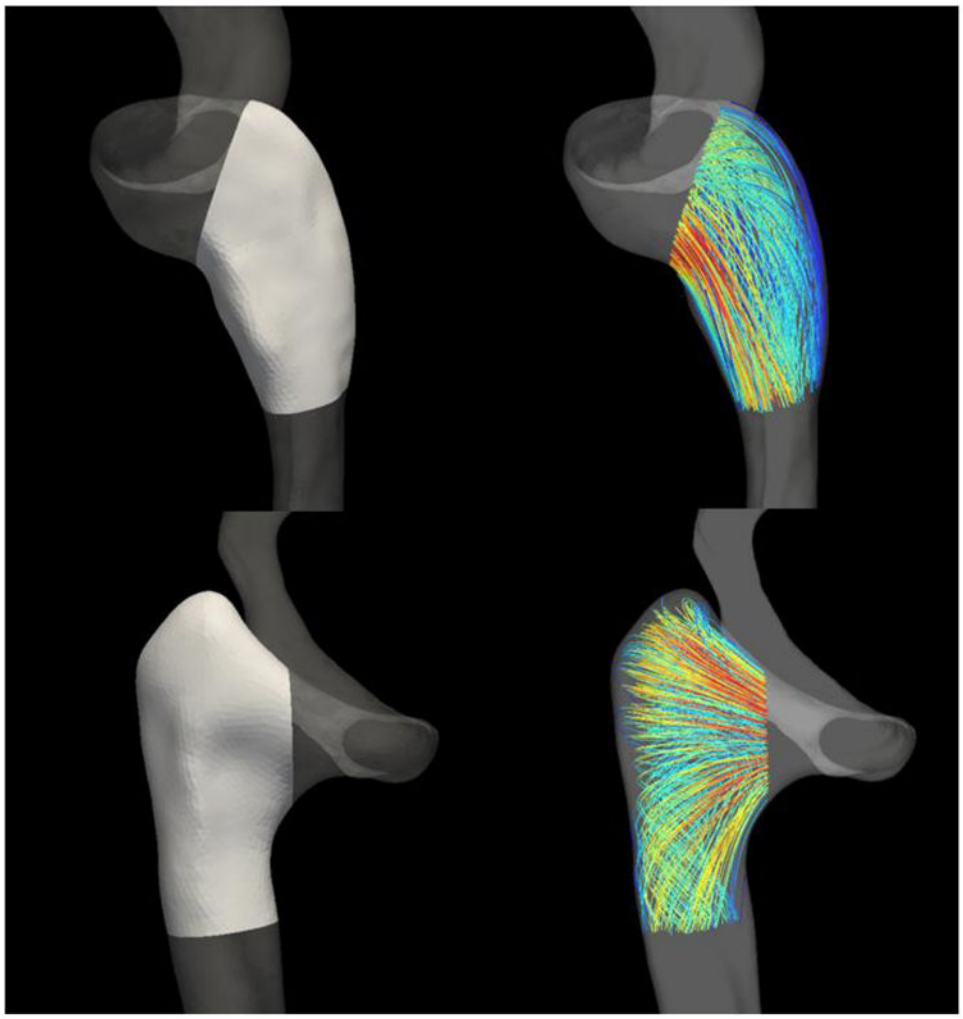

**Figure 2.**

Regions from which streamlines were extracted for calculating the length-averaged streamline curvature (about 1.5 cm along the centerline). These regions were carefully chosen to include only the flow within the proximal internal jugular vein. **Top Row**: A rounded bulb geometry. **Bottom Row**: An elevated bulb geometry.

Author Manuscript Author Manuscript Author Manuscript Author Manuscript

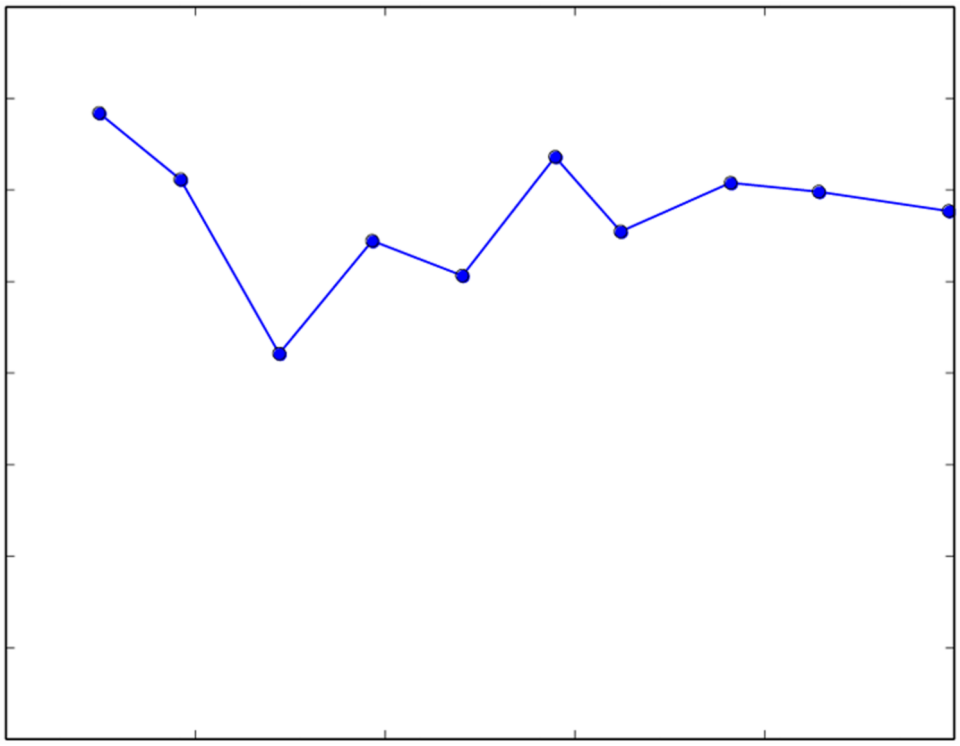

**Figure 3.**
Calculated values of $C$ for specific values of $N$ for a single subject. In this study, $N$ was typically chosen to be in the range of 800-1000 in order to reduce the effect that random streamline seed points had on the value of $C$.

Author Manuscript Author Manuscript Author Manuscript Author Manuscript

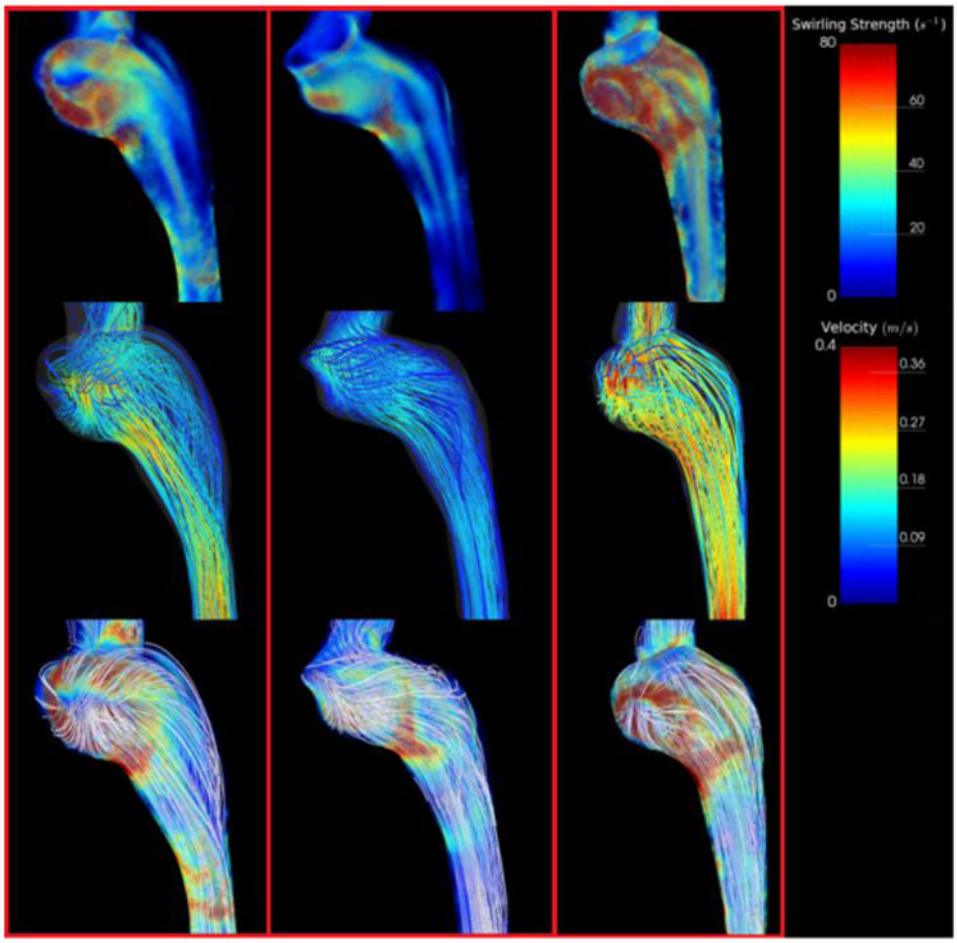


**Figure 4.**

Simulation results depicting swirling strength and streamlines for all subjects with rounded jugular bulbs. **Top Row**: Swirling strength distributions throughout the jugular vein representing regions of vortical flow. Note the presence of strong (red) vortex cores in the jugular bulb parallel to flow. **Middle Row**: Streamlines representing the flow field within the jugular vein. Note that most streamlines from the sigmoid sinus fall straight into the internal jugular vein. **Bottom Row**: Streamlines visualized with swirling strength. Streamlines are uncolored to emphasize secondary flow structures.

Author Manuscript Author Manuscript Author Manuscript Author Manuscript

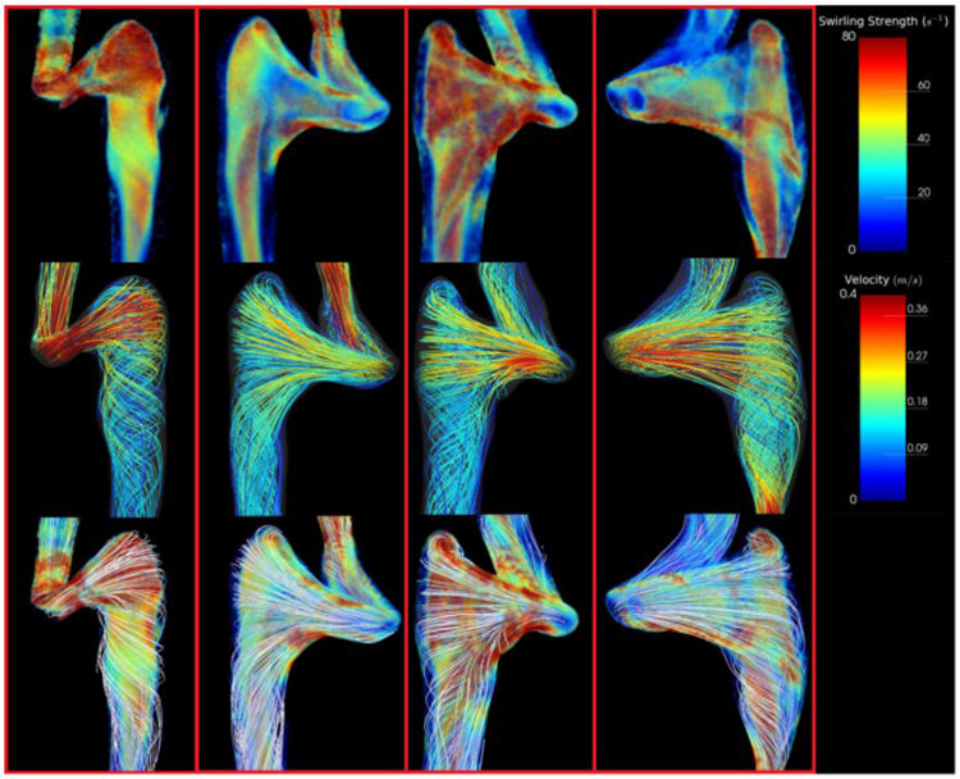


**Figure 5.**

Simulation results depicting swirling strength and streamlines for all subjects with elevated jugular bulbs. **Top Row**: Swirling strength distributions throughout the jugular vein representing regions of vortical flow. Note the presence of a large vortex core encompassing the nearly the entire volume of the proximal jugular vein. **Middle Row**: Streamlines representing the flow field within the jugular vein. Note that most streamlines have a significant component that is perpendicular to the direction of flow. **Bottom Row**: Streamlines visualized with swirling strength. Note the outermost streamlines encircling the prominent vortex core.

Author Manuscript Author Manuscript Author Manuscript Author Manuscript

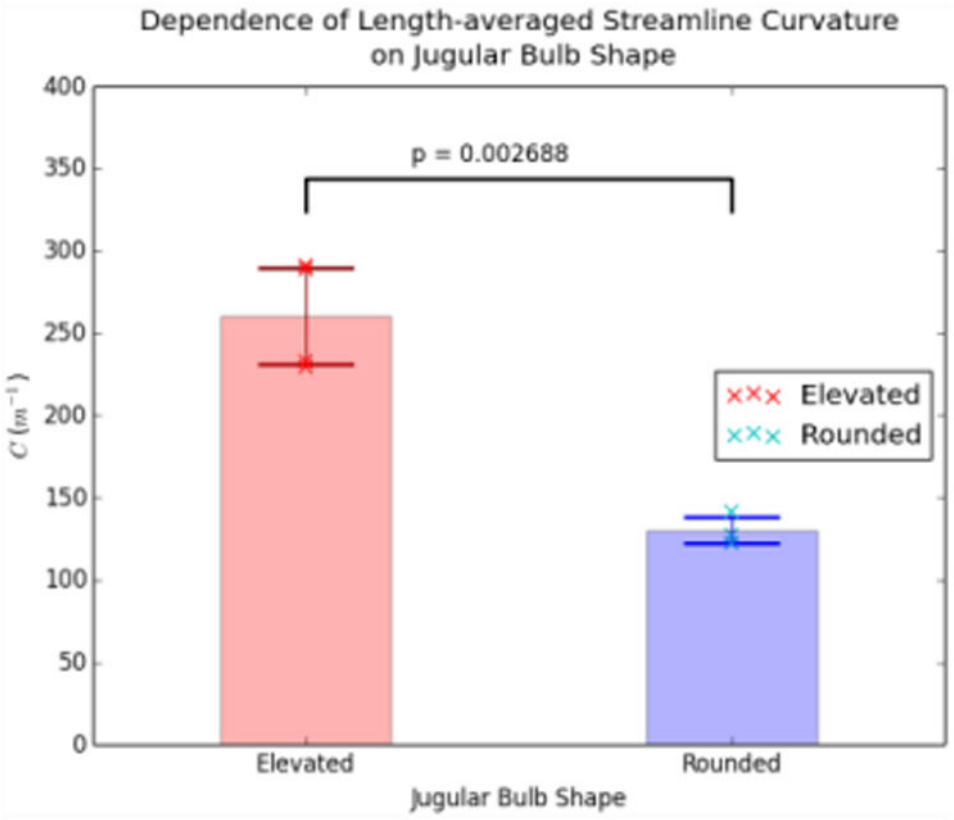


**Figure 6.**

Comparison of $C$ for Elevated and Rounded geometries. The cross marks represent values of $C$ for individual subjects, while the transparent bars and associated error bars represent the mean and standard deviation, respectively.

Author Manuscript Author Manuscript Author Manuscript Author Manuscript

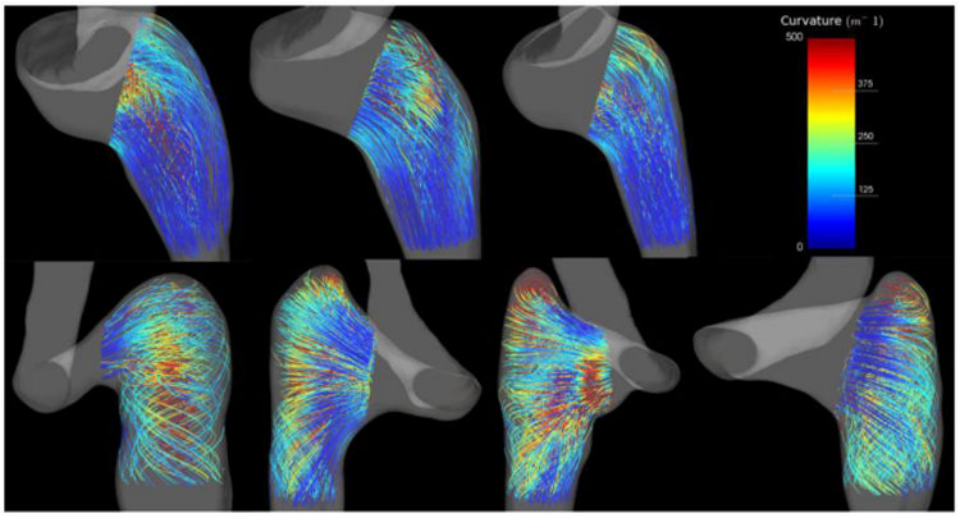


**Figure 7.**

Streamlines in the region of interest colored by curvature. **Top Row**: Rounded jugular bulbs. **Bottom Row**: Elevated jugular bulbs.

Author Manuscript

Author Manuscript

Author Manuscript

Author Manuscript

## Table 1

Number of subjects recruited and the distributions into subgroups. Only the shaded subgroups (Elevated, Rounded) were included in the CFD analysis and compared to one another.

| | | Subjects | Controls |
|---|---|---|---|
| | **Total Recruited** | **12** | **4** |
| Exclusion criteria | Known underlying PT pathology | 2 | 0 |
| | Deafness | 1 | 0 |
| | Neither | 6 | 0 |
| Bulb geometry | Elevated | 3 | 1 |
| | Rounded | 0 | 3 |

Author Manuscript

Author Manuscript

Author Manuscript

Author Manuscript

## Table 2

A comparison of flow-related parameters between the control and patient groups. Only subjects that were included per Table 1 were used in these calculations. The hydraulic diameter was calculated as 4*Area/Perimeter. P-values show that the mean and systolic flow values as well as the corresponding Reynolds numbers between the two groups were not statistically significant.

| | Controls | Subjects | P |
|---|---|---|---|
| Number of Subjects | 4 | 3 | |
| Area ($m^2$) | $6.47 \pm 3.12 \times 10^{-5}$ | $5.91 \pm 2.85 \times 10^{-5}$ | |
| Perimeter (m) | $2.87 \pm 0.78 \times 10^{-3}$ | $2.79 \pm 0.81 \times 10^{-3}$ | |
| Hydraulic Diameter (m) | $8.54 \pm 2.53 \times 10^{-3}$ | $8.06 \pm 2.15 \times 10^{-3}$ | |
| Mean Flow (mL $s^{-1}$) | 4.53 ± 0.74 | 4.61 ± 2.11 | 0.953 |
| Peak Flow (mL $s^{-1}$) | 5.63 ± 1.26 | 5.95 ± 2.24 | 0.834 |
| $Re_{mean}$ | 205 ± 75 | 199 ± 59 | 0.914 |
| $Re_{peak}$ | 254 ± 100 | 267 ± 91 | 0.871 |